SUPPORTING INFORMATION

Dual Reaction Channels for Photocatalytic Oxidation of Phenylmethanol on Anatase

Ye-Fei Li, Zhi-Pan Liu*

Shanghai Key Laboratory of Molecular Catalysis and Innovative Materials, Department of Chemistry, Key Laboratory of Computational Physical Science (Ministry of Education), Fudan University, Shanghai 200433, China * Fax: (+86) 21-6564-2400; E-mail address: zpliu@fudan.edu.cn (Z.-P. Liu).

1. DFT/CM-MPB methods and surface models

All DFT calculations were first performed using SIESTA[1, 2] where optimized double-ζ plus polarization numerical atomic orbital basis sets[3] were utilized along with the Troullier-Martins norm-conserving pseudopotentials.[4] The exchange correlation functional utilized is at the generalized gradient approximation level proposed by Perdew, Burke and Ernzerhof (GGA-PBE)[5]. The semi-core 3s and 3p states of Ti were included in all calculations. The cutoff for the real space grid was set as 150 Ry. The L-BFGS method was employed for geometry relaxation until the maximal forces on each relaxed atom were less than 0.1 eV/Å. All transition states (TSs) of reaction were searched using Constrained-Broyden-Minimization and Constrained-Broyden-Dimer methods designed for treating complex reaction systems[6-8].

Because pure DFT functionals have well-known deficiency in estimating the band gap of semiconducting materials, such as TiO_2, the CP2K/QUICKSTEP[9] package was utilized to verify the role of density functional on reaction kinetics. In CP2K, the hybrid functionals, such as HSE06, are available for treating large oxide surface systems thanks to the auxiliary density matrix method[10] for computing the Hartree-Fock exchange. The calculated band gap using above setups are 2.35, 3.60 eV from PBE and HSE06 functionals, respectively, which are consistent with previous work.[11, 12] In contrast to the large effect of functional on the band gap, we found that the difference in the calculated barrier is generally small (e.g. the barriers of the C-H cleavage in the presence of a hole differ less than 0.1 eV using the two functionals).

The solid-liquid interface is modeled using a recently-developed periodic CM-MPB method[13-15], which can account for the long-range electrostatic interaction due to solvation between surface and solution. Using the approach, the surface can be charged to mimic the charged surface under photocatalytic conditions and the counter charge is distributed as point charges outside the surface (the vacuum region) in the manner determined by the MPB equation. Such a distribution mimics the realistic electrolyte distribution and is thus more physically meaningful compared to the homogeneous background charge in standard periodic DFT calculation[16]. We have recently utilized this approach for modeling electrochemical reaction on metal surfaces[17] and a detailed description on the methodology can be found in our recent work[18]. In this work, the dielectric constants of bulk solution are set as ε_∞ = 78.36 for aqueous solution. Within the CM-MPB framework, it is convenient to align the band position of extended surfaces with the same solution level (e.g., ~15 Å away from the surface).

The anatase (101) surface is modeled using a rectangular unit cell of six TiO_2 layer slab (10.398 × 15.264 Å, $(TiO_2)_{96}$, 288 atoms) with the vacuum spacing being generally larger than 30 Å. In all calculations, the central two TiO_2 layers are fixed at bulk-truncated positions while the other layers are allowed to relax. Due to the large unit cell, only Γ-point was utilized. The

convergence of the k-point mesh and basis set in calculating the barrier has been checked for key reactions (the barrier difference for the C-H cleavage of phenylmethanol is < 0.1 eV on going from Γ-point to (5×3×1) k-point mesh). Furthermore, these DFT calculation setups have been carefully benchmarked with plane-wave methods. For instance, the calculated barrier of C-H cleavage with net charge (+1|*e*|, a four-layer TiO_2 slab in vacuum, two bottom layers fixed at bulk-truncated positions) are 0.38 eV from plane-wave methods and 0.33 eV from SIESTA, respectively.

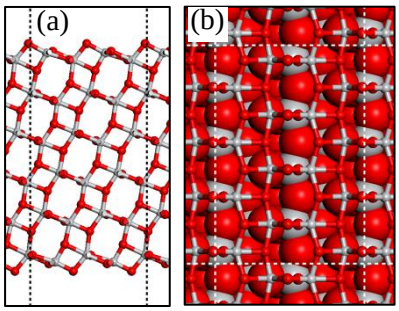

S-Fig 1. The side (a) and top (b) view of the anatase (101) slab utilized in this work. Ti, gray; O, red.

2. Theoretical approach for calculating the kinetics of photocatalytic reactions

To treat photocatalytic kinetics on solid surfaces, a most practical approach is to focus on the electron/hole driven redox chemistry, assuming that after the separation of the photo-generated exciton and concomitant intra-band deexcitation has taken place. This is reasonable as the temporal scale for electron relaxation is ~fs, being much shorter than that for charge recombination (>10 ns in anatase).[19] With this assumption, the surface redox chemistry can be considered as the surface reaction occurring in the presence of an excess electron or hole at the solid-liquid interface. This reduces the computational task to model appropriately the charged (not "excited-state") systems. In this work, the DFT/CM-MPB method is used to calculate the charged surface systems.

Specifically, for a photocatalytic reaction, such as HA dissociation into A and H^+ (HA + h^+ → A + H^+), we can decompose the reaction into three elementary steps, (i) the charging of an adsorbed HA molecule on surface (HA/sur) by a photo-generated hole, HA/sur + h^+ → $[HA/sur]^+$; (ii) the chemical bond breaking by overcoming a TS $[H\text{---}A/sur]^+$, $[HA/sur]^+$ →A + $[H/sur]^+$; (iii) the adsorbed H in $[H/sur]^+$ desorbs to the solution, i.e. $[H/sur]^+$ → sur +H^+(aq). The free energy change ΔG of the three steps can be deduced as ΔG_1, ΔG_2 and ΔG_3, and the free energy barrier ΔG_a of the second step can be calculated by locating the TS of AH dissociation in the presence of a surface hole.

$$\Delta G_1 = G([HA/sur]^+) + G(sur) - G(sur^+) - G(HA/sur) \quad (1)$$

$$\Delta G_2 = G([A+H/sur]^+) - G([HA/sur]^+) \quad (2)$$

$$\Delta G_a = G([H\text{---}A/sur]^+) - G([HA/sur]^+) \quad (3)$$

$$\Delta G_3 = G(H^+_{aq}) + G(A/sur) - G([A+H/sur]^+) \quad (4)$$

The ΔG of HA + h^+ → A + H^+ can be written as

$$\Delta G = \Delta G_1 + \Delta G_2 + \Delta G_3 \quad (5)$$

By utilizing the SHE reference electrode:

$$\Delta G_{SHE} = 1/2G(H_2) - G(H^+_{aq}) + 4.6\ eV = 0 \quad (6)$$

We can obtain the overall free energy change as

$$\Delta G = G(A/sur) + 1/2G(H_2) - G(HA/sur) - (G(sur^+) - G(sur) - 4.6\ eV) \quad (7)$$

This is equivalent to the overall free energy change by using thermodynamics approach as proposed previously[20] i.e. $\Delta G = G(\mathrm{A/sur}) + 1/2G(\mathrm{H_2}) - G(\mathrm{HA/sur}) - |e|U_h$. The term ($G(\mathrm{sur}^+) - G(\mathrm{sur}) - 4.6$ eV) is exactly the electrostatic potential of hole (U_h) at VBM vs. SHE. Obviously, to obtain the kinetics correctly, a realistic estimation of VBM and CBM is a must (otherwise the computed reaction barrier will be incorrect due to the wrong chemical potential of hole/electron). In this work, we utilize a charged-slab method to estimate VBM and CBM, which has been addressed in the Appendix section.

Reference

1. **J. M. Soler, E. Artacho, J. D. Gale, A. García, J. Junquera, P. Ordejón and D. Sánchez-Portal, *J. Phys.: Condens. Matter*, 2002, 14, 2745.**
2. **D. Sánchez-Portal, P. Ordejón, E. Artacho and J. M. Soler, *Int. J. Quantum Chem.*, 1997, 65, 453-461.**
3. **J. Junquera, Paz, Oacute, scar, aacute, D. nchez-Portal and E. Artacho, *Phys. Rev. B*, 2001, 64, 235111.**
4. **N. Troullier, J. Martins, eacute and Luriaas, *Phys. Rev. B*, 1991, 43, 1993.**
5. **J. P. Perdew, K. Burke and M. Ernzerhof, *Phys. Rev. Lett.*, 1996, 77, 3865.**
6. **H.-F. Wang and Z.-P. Liu, *J. Am. Chem. Soc.*, 2008, 130, 10996-11004.**
7. **C. Shang and Z.-P. Liu, *J. Chem. Theory Comput.*, 2010, 6, 1136-1144.**
8. **C. Shang and Z.-P. Liu, *J. Chem. Theory Comput.*, 2012, 8, 2215-2222.**
9. **J. VandeVondele, M. Krack, F. Mohamed, M. Parrinello, T. Chassaing and J. Hutter, *Comput. Phys. Commun.*, 2005, 167, 103-128.**
10. **M. Guidon, J. r. Hutter and J. VandeVondele, *J. Chem. Theory Comput.*, 2010, 6, 2348-2364.**
11. **M. E. A.-d. Dompablo, A. Morales-Garcia and M. Taravillo, *The Journal of Chemical Physics*, 2011, 135, 054503-054509.**
12. **F. Labat, P. Baranek, C. Domain, C. Minot and C. Adamo, *The Journal of Chemical Physics*, 2007, 126, 154703.**
13. **J. L. Fattebert and F. Gygi, *Phys. Rev. B*, 2006, 73, 115124.**
14. **J.-L. Fattebert and F. Gygi, *Int. J. Quantum Chem.*, 2003, 93, 139-147.**
15. **H.-F. Wang and Z.-P. Liu, *The Journal of Physical Chemistry C*, 2009, 113, 17502-17508.**
16. **M. K. Y. Chan and G. Ceder, *Phys. Rev. Lett.*, 2010, 105, 196403.**
17. **Y.-H. Fang and Z.-P. Liu, *J. Am. Chem. Soc.*, 2010, 132, 18214-18222.**
18. **Y.-H. Fang, G.-F. Wei and Z.-P. Liu, *Catal. Today*.**
19. **M. Xu, Y. Gao, E. M. Moreno, M. Kunst, M. Muhler, Y. Wang, H. Idriss and C. Wöll, *Phys. Rev. Lett.*, 2011, 106, 138302.**
20. **Y.-F. Li, Z.-P. Liu, L. Liu and W. Gao, *J. Am. Chem. Soc.*, 2010, 132, 13008-13015.**

3. Structures and energetics of reaction pathways

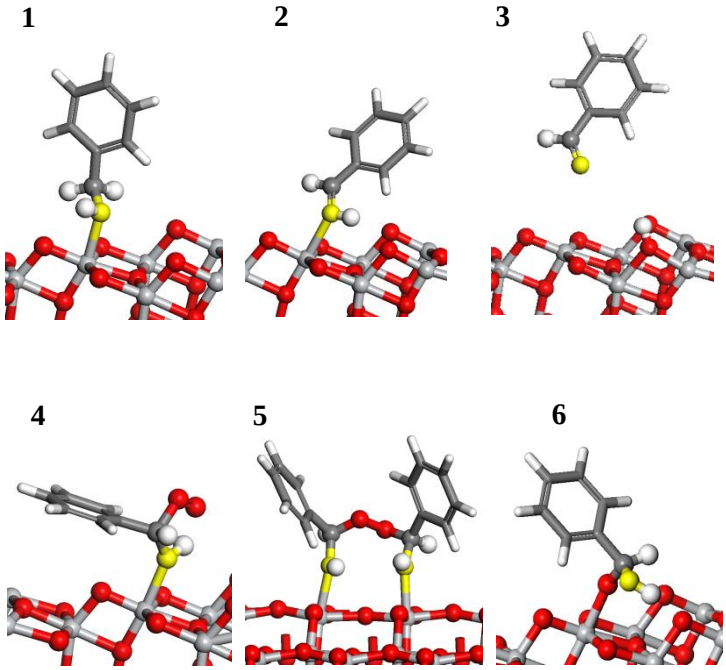

S-Fig. 2. The structures of the optimized reaction intermediates. 1: $C_6H_5CH_2OH$*; 2: C_6H_5CHOH*; 3: C_6H_5CHO(aq)+H*; 4: $C_6H_5CH(OO)OH$*; 5: $[C_6H_5CH(OH)O]_2$*; 6: $C_6H_5CH(OH)O$*. Ti, gray; O, red/yellow (yellow for highlighting the O in alcohol); H, white; C, dark gray.

S-Table 1. The free energy (eV) profiles for the monomer and dimer pathways in aqueous surroundings (R= C_6H_5)

elementary steps*	ΔE	$\Delta H_{(0\rightarrow 298K)}$	ΔZPE	-TΔS	ΔG
		monomer pathway			
IS→1	-0.63	0	0.04	0	-0.59
1→2	-1.82	0.04	-0.17	-0.20	-2.15
2→3	-0.30	0	-0.04	0	-0.34
3→FS	-3.11	0.04	-0.17	-0.20	-3.44
		dimer pathway			
IS→1	-0.63	0	0.04	0	-0.59
1→2	-1.82	0.04	-0.17	-0.20	-2.15
2→4	-0.54	-0.04	0.03	0.32	-0.23
4→5	-0.97	0	0.03	0	-0.94
5→6	-0.45	0.03	-0.09	-0.24	-0.75
6→FS	-0.87	0.03	-0.06	-0.24	-1.14

* **IS→1:** $RCH_2OH(aq) + * \rightarrow RCH_2OH*$;
1→2: $RCH_2OH* + h^+ \rightarrow RCHOH* + H^+(aq)$;
2→3: $RCHOH* \rightarrow RCHO(aq) + H*$;
3→FS: $H*+ h^+ \rightarrow H^+(aq) + *$;
2→4: $1/2RCHOH* + 1/2O_2(g) \rightarrow 1/2RCH(OO)OH*$;
4→5: $1/2RCH(OO)OH* + 1/2RCHOH* \rightarrow 1/2[RCH(OH)O]_2*$;
5→6: $1/2[RCH(OH)O]_2* + 1/2e^- + 1/2H^+(aq) \rightarrow 1/2RCHO(aq) + 1/2H_2O(aq) + 1/2RCHOHO*$;
6→FS: $1/2RCH(OH)O*+1/2e^- + 1/2H^+(aq) \rightarrow 1/2RCHO(aq) + 1/2H_2O(aq) + *$

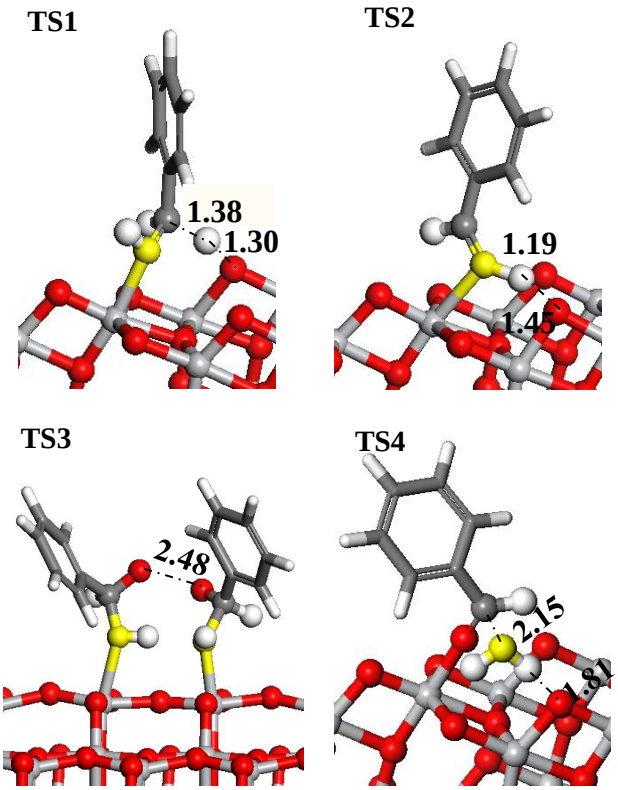

S-Fig. 3. The optimized structures of TSs. **TS1**: TS for $C_6H_5CH_2OH^+$*→ C_6H_5CHOH* + H^+*; **TS2**: TS for C_6H_5CHOH*→C_6H_5CHO(aq)+H*; **TS3**: TS for $[C_6H_5CH(OH)O]_2^-$* → C_6H_5CHO(aq) + OH^-* + $C_6H_5CH(OH)O$*; **TS4**: TS for C_6H_5CHOHO* + H* → C_6H_5CHO(aq) + H_2O(aq) + *. The key distances (Å) at the TSs are labeled in the figure. Ti, gray; O, red/yellow (yellow for highlighting the O in alcohol); H, white; C, dark gray.

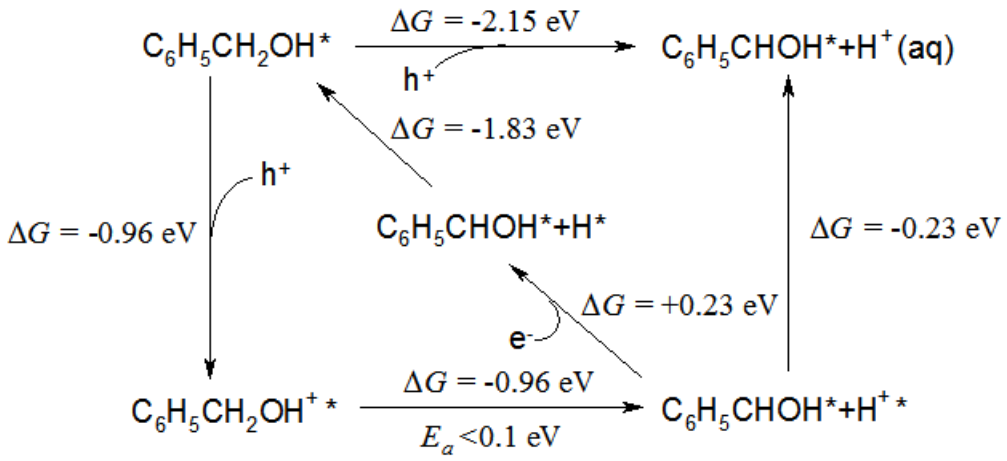

S-Scheme 1. The free energy diagram for the CH bond breaking of phenylmethanol

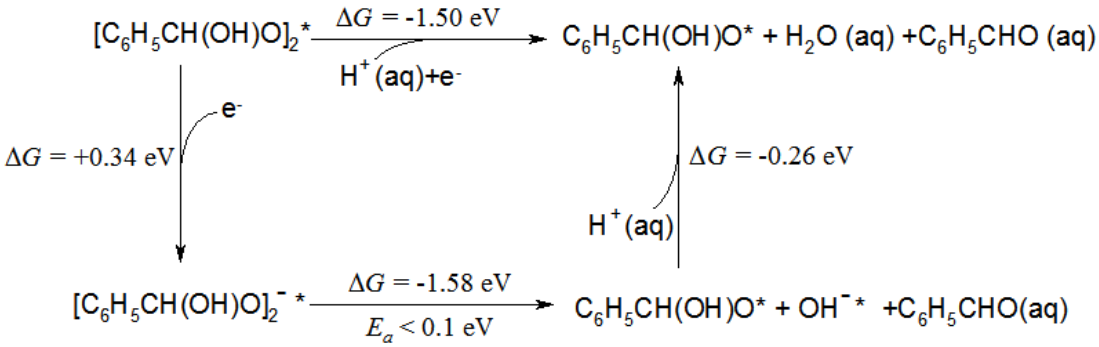

S-Scheme 2. The free energy diagram for the decomposition of $[C_6H_5CH(OH)O]_2$.

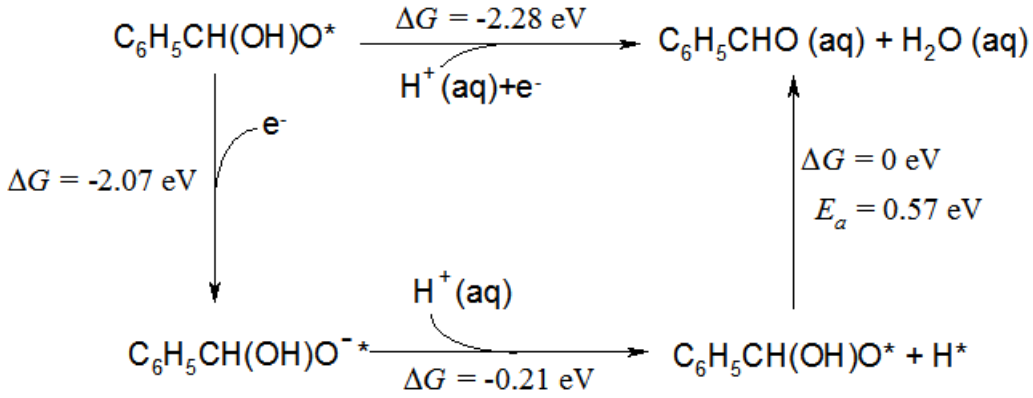

S-Scheme 3. The free energy diagram for the decomposition of $C_6H_5CH(OH)O^*$.